J. Am. Chem. Soc. **2000,** *122,* 12334−12339

Functionalization of Diamond(100) by Cycloaddition of Butadiene: First-Principles Theory

Danesha R. Fitzgerald and Douglas J. Doren*

Contribution from the Department of Chemistry and Biochemistry, University of Delaware, Newark, Delaware 19716

Received June 6, 2000. Revised Manuscript Received October 20, 2000

Abstract: Density functional theory calculations have been used to study [4+2] and [2+2] cycloaddition reactions between 1,3-butadiene and the diamond(100) surface. The structure, energetics, and spectra of the products, as well as the reaction pathways and activation barriers, are discussed. The [4+2] product is energetically favored over the [2+2] product, and the barrier to [4+2] addition is lower than that to [2+2] addition, so the [4+2] product is expected to be the dominant product on the surface. Interdimer interactions influence the structure and vibrational spectrum of the [4+2] product, but have a small effect on the adsorption energy. Comparisons to experimental studies are made, and while the [4+2] product appears to be the major surface species, there is also evidence for the presence of other species.

Introduction

The optical, mechanical, and electronic properties of diamond films make them uniquely suited for a wide range of applications.[1−3] Advances in film growth by chemical vapor deposition (CVD) techniques have made many of these applications feasible. Both the (100) and (111) faces are prevalent in diamond films grown by CVD,[4,5] though the (100) face is more easily grown without defects.[5,6] Diamond(100) films of very high quality have been achieved through CVD methods[1] and these films have been successfully used in the fabrication of electronic devices, where atomically smooth surfaces are essential.[1,2] Beyond simply growing diamond films, it may be useful to make controlled chemical modifications of the diamond surface to tailor its properties for specific applications. Toward this end, we describe theoretical studies of cycloaddition reactions between an unsaturated hydrocarbon (butadiene) and the diamond(100) surface. Similar reactions have been the subject of recent experimental studies on a diamond single crystal[7,8] and an epitaxial diamond film.[9]

The C(100) surface exhibits a 2 × 1 reconstruction in which surface atoms with unsaturated valences pair up to form dimers.[10−13] The bond between the dimer atoms is essentially a strained double bond, with σ and π components. This suggests that the surface may react toward small organic molecules very much like a molecular carbon−carbon double bond. This paper addresses two types of elementary cycloaddition reactions that might occur between a 1,3-diene and the surface dimer (Scheme 1): [4+2] cycloaddition (the Diels−Alder reaction) and [2+2] cycloaddition.

Scheme 1

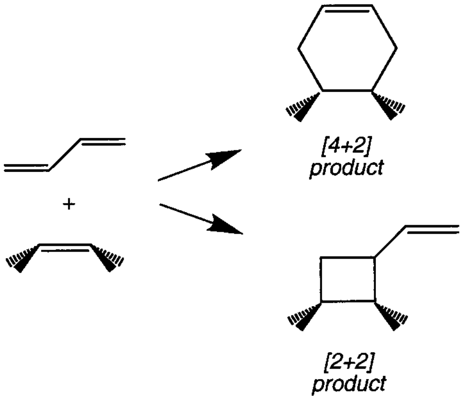

Several chemical precedents provide a guide to understanding these surface reactions. The [4+2] cycloaddition is widely applied to molecular C−C double bonds, but if the activation energy on a diamond surface is as high as that for a molecular double bond (typically 20 kcal/mol or more[14−18]) the reaction probability will be negligibly small in the ultrahigh vacuum conditions required for surface studies. However, the surface dimer bond is weaker than molecular C−C π-bonds: bonds to

---

[1] Flöter, A.; Guttler, H.; Schulz, G.; Baumann, R.; Lutz-Elsner, C.; Zachai, R.; Gluche, P.; Adamschik, M.; Aleksov, A.; Kohn, O.; Ebert, W.; Kohn, E.; Nebel, C. E.; Rohrer, E. *Diamond Films Technol.* **1998**, *8*, 299.

[2] Ashfold, M. N. R.; May, P. W.; Rego, C. A.; Everitt, N. M. *Chem. Soc. Rev.s* **1994**, *23*, 21.

[3] *MRS Bulletin*; Fleischer, E. L., Ed.; 1998; p 23.

[4] Winn, M. D.; Rassinger, M.; Hafner, *J. Phys. Rev. B* **1997**, *55*, 5364.

[5] Yang, Y. L.; Struck, L. M.; Sutcu, L. F.; D'Evelyn, M. P. *Thin Solid Films* **1993**, *225*, 203.

[6] Hukka, T. I.; Pakkanen, T. A.; D'Evelyn, M. P. *J. Phys. Chem.* **1994**, *98*, 12420.

[7] Hovis, J. S.; Coulter, S. K.; Hamers, R. J.; D'Evelyn, M. P.; Russell, J. N., Jr.; Butler, J. E. *J. Am. Chem. Soc.* **2000**, *122*, 732.

[8] Wang, G. T.; Bent, S. F.; Russell, J. N.; Butler, J. E.; D'Evelyn, M. P. *J. Am. Chem. Soc.* **2000**, *122*, 744.

[9] Hossain, M. Z.; Aruga, T.; Takagi, N.; Tsuno, T.; Fujimori, N.; Ando, T.; Nishijima, M. *Jpn. J. Appl. Phys.* **1999**, *38*, L1496.

[10] Furthmüller, J.; Hafner, J.; Kresse, G. *Phys. Rev. B* **1996**, *53*, 7334.

[11] Yang, C.; Kang, H. C. *J. Chem. Phys.* **1999**, *110*, 11029.

[12] Weiner, B.; Skokov, S.; Frenklach, M. *J. Chem. Phys* **1995**, *102*, 5486.

[13] Yang, C.; Kang, H. C. *Surf. Sci.* **1998**, *409*, 521.

[14] Houk, K. N.; Li, Y.; Evanseck, J. D. *Angew. Chem., Int. Ed. Engl.* **1992**, *31*, 682.

[15] Goldstein, E.; Beno, B.; Houk, K. N. *J. Am. Chem. Soc.* **1996**, *118*, 6036.

[16] Borden, W. T.; Loncharich, R. J.; Houk, K. N. *Annu. Rev. Phys. Chem.* **1988**, *39*, 213.

[17] Bernardi, F.; Bottoni, A.; Robb, M. A.; Schlegel, H. B.; Tonachini, G. *J. Am. Chem. Soc.* **1985**, *107*, 2260.

[18] Li, Y.; Houk, K. N. *J. Am. Chem. Soc.* **1993**, *115*, 7478.

10.1021/ja002023j CCC: $19.00

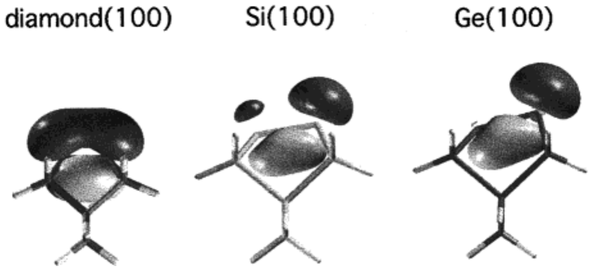

Figure 1. Natural bond orbitals [ref 19] corresponding to the dimer π bond on single-dimer cluster models of diamond(100), Si(100), and Ge(100).

subsurface atoms necessarily impose a nonplanar geometry on the dimer, which causes poor overlap between the atomic orbitals that contribute to the π-bond (Figure 1). The diamond(100) dimer π-bond strength is approximately 28 kcal/mol,[6] compared to 56 kcal/mol in ethylene.[20] The weak π-bond in the dimer should lower the reaction barrier to [4+2] cycloaddition, though a quantitative prediction would be useful. On the other hand, the higher reactivity of the surface π-bond may also allow [2+2] cycloaddition (Scheme 1) to compete with [4+2] addition, even though the [2+2] path is not thermally accessible for a typical molecular C$-$C π-bond.[14,17]

These expectations are consistent with experience from Si(100) and Ge(100) surfaces, which exhibit similar 2 × 1 reconstructions.[11,21] On these surfaces, dienes react by the [4+2] mechanism with negligible barriers,[22−26] and alkenes react by [2+2] cycloadditions with low barriers.[27−29] For dienes on Si(100), the [2+2] reaction appears to compete kinetically in some cases to produce a minority side product.[24] However, the π interaction on Si and Ge is even weaker than that on diamond, with a π-bond strength on Si(100) of only 5−10 kcal/mol.[30] This is a consequence of the distance between dimer atoms on Si and Ge, which is almost an angstrom longer than that on diamond. The interaction is so weak on Si(100) and Ge(100) that the lowest energy structure has an asymmetric “buckled” dimer structure, which is quite different from a typical π-bond (Figure 1). A final analogy may be made to the C_{60} and C_{70} fullerenes. Here too, the C$-$C π-bonds are not planar, but (in contrast to diamond) the π-system is conjugated. The nonplanar geometry tends to make the π-bonds more reactive than planar π-bonds, but conjugation of this bond decreases reactivity. Still, fullerenes undergo both [4+2] and [2+2] cycloaddition reactions.[31−35]

A simple consideration of π-bond strengths suggests that the diamond surface dimer will be more reactive than ethylene, but less reactive than Si(100) or Ge(100). This is consistent with recent experiments showing that cyclopentene[7] and butadiene[8,9] each react with the diamond surface, by [2+2] and [4+2] mechanisms, respectively. Apparently both molecules adsorb with a modest barrier. In the case of butadiene, vibrational spectra have been interpreted as evidence for the presence of the [4+2] cycloaddition product on this surface, with possible competition from the [2+2] path to form a minor side product. We present here a complementary theoretical investigation of the structures, energetics, and mechanism of [2+2] and [4+2] cycloadditions of butadiene, and revisit the interpretation of vibrational spectra.

Models and Methods

The density functional theory calculations[36] presented here used the B3LYP functional, which consists of the Becke three-parameter exchange functional and the Lee, Yang, and Parr correlation functional.[37,38] The B3LYP functional has been used to predict accurate activation barriers for cycloaddition reactions to molecular C$-$C double bonds.[15,39] It was also used in the original prediction that the Diels−Alder reaction would proceed without an activation barrier on Si(100),[22] a fact that has since been well-established experimentally.[24,26] The analogous reaction on Ge(100) is reversible,[40] and the measured desorption activation energy agrees well with theory.[41]

A 6-31+G* basis set was used to optimize all critical points on the potential energy surface. The Hessian matrix of second derivatives was calculated at each critical point to verify that they were either true minima or first-order saddle points, and to provide zero-point energy corrections and vibrational spectra. The calculated frequencies have been scaled by a factor of 0.955, a value that we have found to be effective for scaling vibrational frequencies in several problems. Minimizations were done from each transition state to identify the reactants and products that lie on each side of the saddle point. Single-point calculations were done at selected critical points using the 6-311+G* and 6-311++G** basis sets to investigate the effect on the reaction energetics. Reported energies are zero-point corrected, unless otherwise noted. Wave function stability was tested for all structures suspected of having diradical character.

Two cluster models were used to represent the C(100)-2 × 1 surface. A C_9H_{12} cluster represents a single surface dimer; a $C_{21}H_{20}$ cluster represents three adjacent surface dimers from a single dimer row. Comparison of these models shows how adjacent unreacted dimers would affect product formation. In each model, the valences of the subsurface carbons were saturated by hydrogen atoms. No constraints

---

(19) Glendening, E. D.; Badenhoop, J. K.; Reed, A. E.; Carpenter, J. E.; Weinhold, F. *NBO 4.0*; Theoretical Chemistry Institute, University of Wisconsin: Madison, WI, 1996.

(20) McMurry, J. *Organic Chemistry*, 4th ed.; Brooks/Cole Publishing Company: Pacific Grove, 1996; pp 23−24.

(21) Krüger, P.; Pollmann, J. *Phys. Rev. Lett.* **1995**, *74*, 1155.

(22) Konecny, R.; Doren, D. J. *J. Am. Chem. Soc.* **1997**, *119*, 11098. Konecny, R.; Doren, D. J. *Surf. Sci.* **1998**, *417*, 169.

(23) Lee, S. W.; Nelen, L. N.; Ihm, H.; Scoggins, T.; Greenlief, C. M. *Surf. Sci.* **1998**, *410*, L773.

(24) Hovis, J. S.; Liu, H.; Hamers, R. J. *J. Phys. Chem. B* **1998**, *102*, 6873.

(25) Wang, G. T.; Mui, C.; Musgrave, C. B.; Bent, S. F. *J. Phys. Chem. B* **1999**, *103*, 6803.

(26) Teplyakov, A. V.; Kong, M. J.; Bent, S. F. *J. Am. Chem. Soc.* **1997**, *119*, 11100. Teplyakov, A. V.; Kong, M. J.; Bent, S. F. *J. Chem. Phys.* **1998**, *108*, 4599.

(27) Yoshinobu, J.; Tsuda, H.; Onchi, M.; Nishijima, M. *J. Chem. Phys.* **1987**, *87*, 7332.

(28) Cheng, C. C.; Wallace, R. M.; Taylor, P. A.; Choyke, W. J.; Yates, J. T., Jr. *J. Appl. Phys.* **1990**, *67*, 3693.

(29) Hamers, R. J.; Hovis, J. S.; Lee, S.; Liu, H.; Shan, J. *J. Phys. Chem. B* **1997**, *101*, 1489.

(30) Doren, D. J. *Adv. Chem. Phys.* **1996**, *95*, 1.

(31) Mestres, J.; Duran, M.; Solà, M. *J. Phys. Chem.* **1996**, *100*, 7449.

(32) Giovane L. M.; Barco, J. W.; Yadav, T.; Lafleur, A. L.; Marr, J. A.; Howard, J. B.; Rotello, V. M. *J. Phys. Chem.* **1993**, *97*, 8560.

(33) Rubin, Y.; Khan, S.; Freedberg, D. I.; Yeretzian, C. *J. Am. Chem. Soc.* **1993**, *115*, 344.

(34) Wudl, F. *Acc. Chem. Res.* **1992**, *25*, 157.

(35) Shvartsburg, A. A.; Pederson, L. A.; Hudgins, R. R.; Schatz, G. C.; Jarrold, M. F. *J. Phys. Chem. A* **1998**, *102*, 7919.

(36) Frisch, M. J.; Trucks, G. W.; Schlegel, H. B.; Scuseria, G. E.; Robb, M. A.; Cheeseman, J. R.; Zakrzewski, V. G.; Montgomery, J. A., Jr.; Stratmann, R. E.; Burant, J. C.; Dapprich, S.; Millam, J. M.; Daniels, A. D.; Kudin, K. N.; Strain, M. C.; Farkas, O.; Tomasi, J.; Barone, V.; Cossi, M.; Cammi, R.; Mennucci, B.; Pomelli, C.; Adamo, C.; Clifford, S.; Ochterski, J.; Petersson, G. A.; Ayala, P. Y.; Cui, Q.; Morokuma, K.; Malick, D. K.; Rabuck, A. D.; Raghavachari, K.; Foresman, J. B.; Cioslowski, J.; Ortiz, J. V.; Stefanov, B. B.; Liu, G.; Liashenko, A.; Piskorz, P.; Komaromi, I.; Gomperts, R.; Martin, R. L.; Fox, D. J.; Keith, T.; Al-Laham, M. A.; Peng, C. Y.; Nanayakkara, A.; Gonzalez, C.; Challacombe, M.; Gill, P. M. W.; Johnson, B.; Chen, W.; Wong, M. W.; Andres, J. L.; Gonzalez, C.; Head-Gordon, M.; Replogle, E. S.; Pople, J. A. *Gaussian 98*, revision A.3; Gaussian, Inc.: Pittsburgh, PA, 1998.

(37) Lee, C.; Yang, W.; Parr, R. G. *Phys. Rev. B* **1988**, *37*, 785.

(38) Becke, A. D. *J. Chem. Phys.* **1993**, *98*, 1372.

(39) Barone, V.; Arnaud, R. *J. Chem. Phys.* **1997**, *106*, 8727.

(40) Teplyakov, A. V.; Lal, P.; Noah, Y. A.; Bent, S. F. *J. Am. Chem. Soc.* **1998**, *120*, 7377.

(41) Foraker, A. C.; Doren, D. J. Unpublished results.

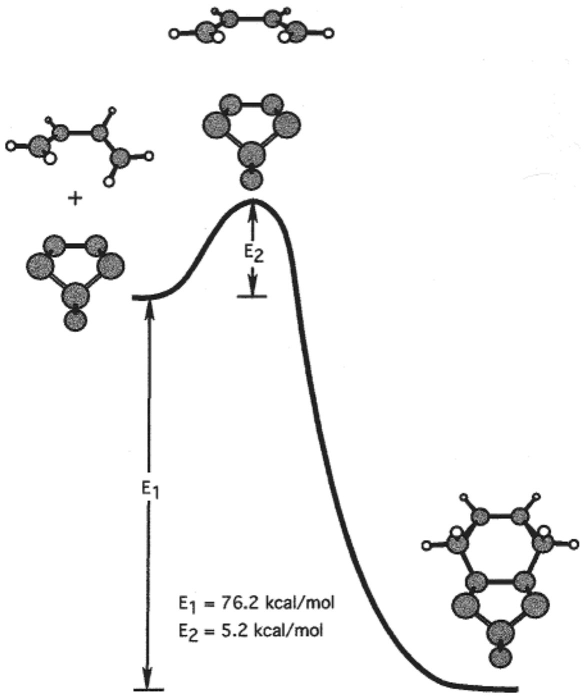

Figure 2. Calculated reaction pathway for the [4+2] cycloaddition of 1,3-butadiene and the single-dimer cluster. Energies are reported with respect to the isolated reactants with butadiene in the less stable cisoid configuration, which is 3.5 kcal/mol higher in energy than the *s-trans* configuration.

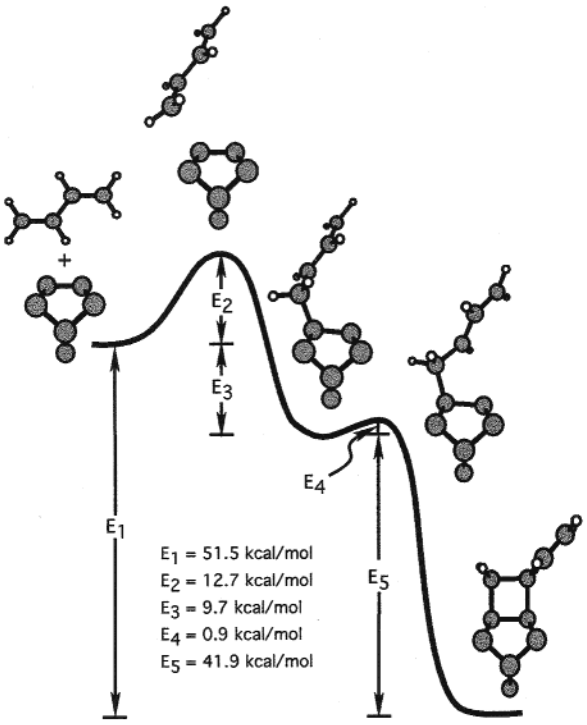

Figure 3. Calculated reaction pathway for the [2+2] cycloaddition of 1,3-butadiene and the single-dimer cluster. Energies are reported with respect to the isolated reactants with butadiene in the *s-trans* configuration.

were imposed on these bare surface models, except that they have C_{2v} symmetry. Similar cluster models have been used before to study the bare surface structure.[12,13] The calculated dimer bond lengths vary only slightly between the models, and they are in good agreement with calculations on a semi-infinite surface model.[21] The reported vibrational frequencies were calculated with deuterium substituted for subsurface hydrogens to isolate the adsorbate C−H stretches.

Results and Discussion

Two cycloaddition reactions are possible between 1,3-butadiene and the dimer atoms of the C(100)-2 × 1 surface. Calculated pathways for the [4+2] and [2+2] reactions on the single-dimer model are shown respectively in Figures 2 and 3. Bond lengths, angles, and energies for critical points on both pathways are reported in Table 1.

Product Structures and Energies. The [2+2] cycloaddition product has a four-member ring, formed from two carbon atoms of the butadiene and the dimer carbons of the surface (Scheme 1). Energy minima were found for both the *s-cis* and *s-trans* conformations of the adsorbate, though the *s-trans* product is slightly more stable, as expected. The *s-trans* adsorbate is bound by 51.5 kcal/mol relative to the separated *s-trans* butadiene and surface, while the *s-cis* product is less than 1 kcal/mol higher in energy. For the *s-trans* product (Figure 4a), the unreacted double bond is bent noticeably away (dihedral angle of 130°) from the planar orientation that is characteristic of isolated *s-trans* butadiene, presumably due to the loss of conjugation. The dimer bond increases from 1.36 Å before reaction to 1.58 Å, consistent with a bond order change from double to single. The reacting butadiene double bond lengthens similarly, while the unreacted butadiene double bond does not change length. A corresponding [2+2] *s-trans* product was found on the three-dimer cluster, with no noticeable difference in adsorbate geometry or binding energy.

The [4+2] product has a six-member ring containing one double bond. The C−C bond lengths are typical of molecular single and double bonds, with the exception of the surface dimer bond, which lengthens considerably, to 1.61 Å, in the product structure. On the single-dimer cluster model, the minimum energy [4+2] cycloaddition product has C_s symmetry with a bent ring structure, with the plane defined by the butadiene carbons noticeably bent away from vertical, at an angle of approximately 41° (Figure 4b). This structure is similar to that found on Si(100). A C_{2v} structure, with the ring in a vertical orientation, is a first-order saddle point on the single-dimer model, 2.8 kcal/mol higher than the minimum. However, on the three-dimer cluster model, this vertical structure is the energy minimum (Figure 4c). Apparently, adjacent unreacted dimers have a repulsive interaction with the π-bond of the [4+2] cycloaddition product. This change in angle is the only notable difference between the [4+2] structures on the two cluster models (Table 1). Along with the change in geometry, the [4+2] product binding energy decreases from 76.2 kcal/mol on the one-dimer model to 71.5 kcal/mol on the three-dimer model. Regardless of the surface model, the [4+2] product is energetically favored by 20−25 kcal/mol over the [2+2] product.

Reaction Mechanism. The reaction pathways to the adsorption of butadiene on the C(100)-2 × 1 surface are shown in Figures 2 and 3 for the [4+2] and [2+2] reactions, respectively. The energies shown for the critical points were calculated with the 6-31+G* basis, but single-point energies calculated at critical points on the [4+2] pathway show that energy differences were not noticeably affected by changing to a 6-311+G* or 6-311++G** basis. The [2+2] reaction proceeds through a two-step process (Figure 3). The diradical species along this reaction pathway require unrestricted wave functions in the DFT calculations. The first kinetic barrier is the transition state to formation of one C−C bond with the surface, calculated to be 12.7 kcal/mol with respect to the reactants. The length of the nascent C−C bond is 2.13 Å at this point, while the reacting

Table 1. Bond Lengths, Angles, and Energies for Critical Points on Both the [4+2] and [2+2] Reaction Pathways[a]

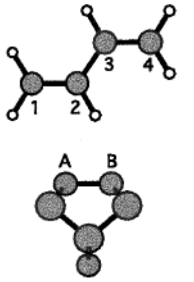

	bond length (Å)							angle (deg)		Δenergy
	A−B	1−2	2−3	3−4	A−1	B−2	B−4	1234	BA12	(kcal/mol)
butadiene (*s-trans*)		1.34	1.46	1.34				180		0.0
butadiene (*s-cis*)		1.34	1.47	1.34				32		3.5
cluster (single-dimer)	1.36									
[4+2] transition state	1.39	1.36	1.44	1.36	2.64		2.64	0	49	8.7
[4+2] product (single-dimer)	1.61	1.51	1.34	1.51	1.54		1.54	0	38	76.2
[4+2] product (three-dimer)	1.59	1.50	1.34	1.50	1.54		1.54	0	0.2	71.5
[2+2] transition state #1	1.43	1.39	1.43	1.36	2.13	3.70		178	57	12.7
[2+2] intermediate	1.57	1.50	1.39	1.39	1.55	3.23		179	62	9.7
[2+2] transition state #2	1.57	1.51	1.40	1.38	1.54	2.63		173	25	8.8
[2+2] product	1.58	1.57	1.50	1.34	1.55	1.58		130	3	51.5

[a] Energies are reported with respect to separated *s-trans* butadiene and bare single-dimer cluster.

butadiene double bond is only slightly longer than in the isolated molecule (Table 1). An intermediate with the first C−C bond fully formed is 41.9 kcal/mol above the products. A negligible barrier (0.9 kcal/mol) must be overcome to form the second C−C bond in the final product.

The [4+2] pathway is concerted, with a symmetric transition state (Figure 2). This was the only transition state found, though searches for asymmetric paths were attempted. The transition state is very early: the dimer−adsorbate C−C distance is 2.64 Å, and the surface dimer and butadiene geometry remain close to the reactant geometries. The activation barrier is 8.7 kcal/mol above the separated *s-trans* butadiene and cluster. To undergo the [4+2] reaction, butadiene must be in the *s-cis* configuration, which is 3.5 kcal/mol higher in energy than the *s-trans* configuration. The barrier in Figure 2 is shown with respect to the *s-cis* configuration, but assuming an equilibrium distribution of *s-cis* and *s-trans* conformers, the competition between the [2+2] and [4+2] paths is determined by the height of the two barriers relative to the most stable (*s-trans*) conformation. Thus, the barrier to the [4+2] reaction is 4 kcal/mol lower than that of the [2+2] reaction.

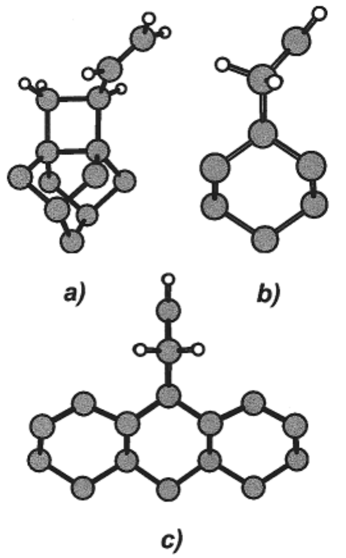

Figure 4. (a) *s-trans* [2+2] product on single-dimer cluster, (b) [4+2] product on single-dimer cluster (side view), and (c) [4+2] product on three-dimer cluster (side view).

Vibrational Spectra. Calculated spectra for [2+2] and [4+2] cycloaddition products can be compared to the experimental infrared spectra of Wang et al. [ref 8] for 1,3-butadiene (Figure 5a) and 1,3-butadiene-*1,1,4,4*-d_4 in the C−H stretch region (Figure 5f). Although the signal-to-noise ratio is low, reasonable agreement is seen between the major peaks in the experimental spectra and the theoretical spectra for the [4+2] bent product. However, there appear to be several peaks in the experimental spectrum between 2880 and 3000 cm^{-1}, while there are only two peaks in this range for the theoretical spectrum of the bent, single-dimer minimum (Figure 5b). On the other hand, the three-dimer model presumably gives a more realistic description of the interactions on an extended surface, and the minimum energy structure on this model is the vertical configuration. For the vertical structure, there are no peaks at all between 2880 and 3000 cm^{-1} (Figure 5c) (spectra calculated for the minimum on the three-dimer model and for the C_{2v} saddle point on the single-dimer model are only slightly different in the C−H stretch region). Thus, the vertical structure, which is expected to be lowest in energy on an extended, defect-free surface, cannot account for many of the prominent spectral features. The bent structure, or some other modified structure, may occur near steps (which are common defects on the diamond surface), and a mixture of the bent and vertical structures would account for more peaks than the vertical structure alone. Still, neither the vertical nor bent [4+2] structures accounts for all the observed peaks. The spectrum of the [2+2] product (Figure 5d) would account for many of the missing peaks. While it appears that the major product on the surface is the [4+2] product, our calculations are consistent with the possibility that the [2+2] product is present as a side product.

Wang et al. also interpreted their spectra as evidence for the [4+2] cycloadduct as the major surface species, with the possibility of a [2+2] side product. Their assignment was primarily based on ruling out the major presence of the [2+2] product by isotope substitution. We have calculated isotope shifts for these structures. The highest frequency peaks in the

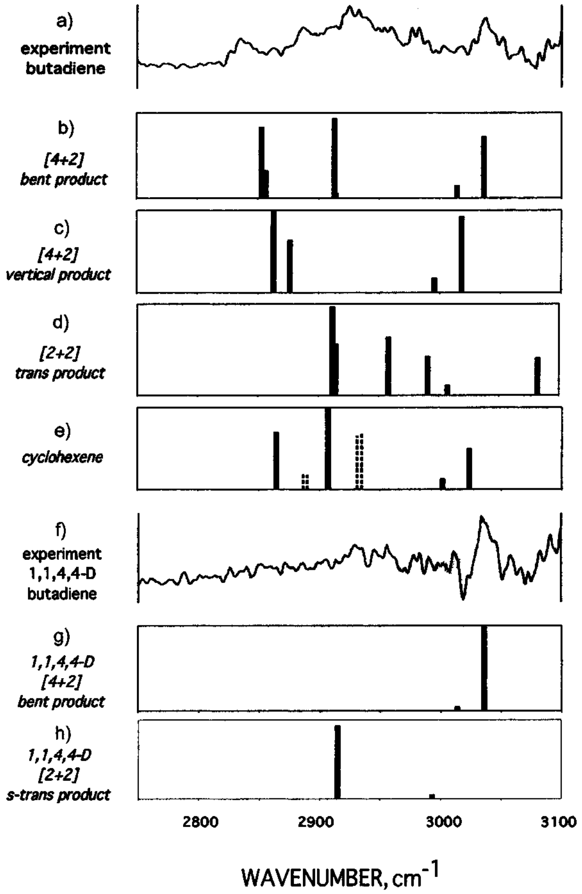

Figure 5. Theoretical and experimental [ref 8] IR spectra of cycloadditions with the diamond(100) surface: (a) experimental 1,3-butadiene, (b) theoretical [4+2] bent product on single-dimer, (c) theoretical [4+2] vertical product on single-dimer, (d) theoretical [2+2] *s-trans* product on single-dimer, (e) theoretical cyclohexene, (f) experimental 1,3-butadiene-*1,1,4,4-d*$_4$, (g) theoretical [4+2] deuterated bent product on single-dimer, and (h) theoretical [2+2] *s-trans* deuterated product on single-dimer.

fully hydrogenated [2+2] product spectrum are attributed to terminal CH_2 stretches on the remaining double bond (Figure 5d); these peaks are red-shifted considerably ($\sim$1000 cm^{-1}) when the terminally deuterated 1,3-butadiene-*1,1,4,4-d*$_4$ is used (Figure 5h). However, in the experimental spectrum of this deuterated species (Figure 5f), the strong high-frequency peak is not shifted, and is consistent with the predicted spectrum of the deuterated [4+2] product (Figure 5g). The spectrum for the deuterated vertical structure (not shown) is similar to that of the bent structure, except that both peaks are red shifted by 18 cm^{-1}. There may also be a weak absorption in the experimental spectrum corresponding to the deuterated [2+2] product, though features in this region are close to the noise level.

Wang et al. have commented on the striking similarity between the IR spectrum of cyclohexene and the adsorbed butadiene. The calculated spectrum for cyclohexene (Figure 5e) appears to agree with the observed spectrum for adsorbed butadiene between 2880 and 3000 cm^{-1} better than that of the [4+2] or [2+2] structures alone, though it also lacks the features at 2950−2975 cm^{-1}. This is hard to understand if the main surface species is the [4+2] cycloadduct, since four peaks (dotted lines in Figure 5e) of the IR spectrum of cyclohexene correspond to C−H stretches that have no analogue in the adsorbed butadiene (four C−H bonds of cyclohexene correspond to C−C back-bonds of the surface dimer). If these “extra” cyclohexene C−H stretches are ignored, the remaining peaks in the cyclohexene spectrum are quite similar to those predicted for our single-dimer bent model.

Scheme 2

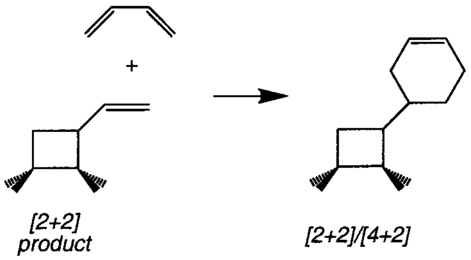

Scheme 3

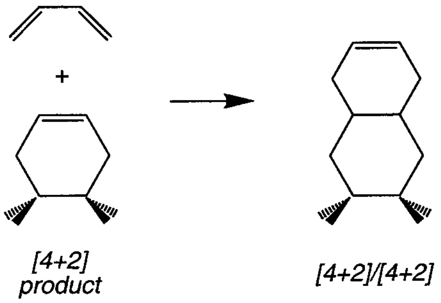

We have considered some alternative reaction sequences that would yield a product with a spectrum similar to that of cyclohexene. One example is [2+2] addition of butadiene to the surface, followed by [4+2] addition of a second butadiene to the initial adduct (Scheme 2). A similar spectrum would also result if initial adsorption by the [4+2] mechanism were followed by [4+2] addition of a second butadiene (Scheme 3). We cannot rule out such species as minor products on the surface, though they are certainly not the dominant product. Neither of the species in Scheme 2 or 3 are likely to be kinetically accessible. Both of the paths involve [4+2] cycloaddition to a molecular C−C double bond, which will have an activation barrier too high for significant reaction probability in the ultrahigh vacuum in which the experiments were performed. Furthermore, the spectrum of the deuterated species is not consistent with either of these species as major products: Both would exhibit intense peaks around 2900 cm^{-1} after deuteration (similar to the deuterated [2+2] addition product), while the only features in this region of the experimental spectrum are close to the noise level.

In summary, a simple way to rationalize the calculated and observed spectra is to propose that the [4+2] product (possibly with more than one conformation) is the dominant species on the surface, but that there may also be a side product, likely the [2+2] product. Definitive assignments of minority species are not possible, however, given the low signal-to-noise ratio of the experimental spectra.

Since the original submission of this paper we have learned of the experiments of Hossain et al.,[9] who used electron energy loss spectroscopy (EELS) to study the adsorption products of 1,3-butadiene on a diamond(100) epitaxial film. They also conclude that the [4+2] product is the major surface species. However, their EELS spectra have relatively low resolution ($\sim$80 cm^{-1}) and do not provide any further insight about adsorbate geometry or the possibility of minority side products. Nevertheless, this experiment clearly shows that the Diels−Alder addition of dienes applies to diamond film surfaces as well as single-crystals.

Conclusions

We have shown detailed reaction pathways for both the [4+2] and [2+2] cycloaddition of 1,3-butadiene with the diamond(100)-2 × 1 surface. The lower activation barrier and more favorable product energy for the [4+2] reaction imply that the [4+2] product will be the dominant surface product. The barrier to [2+2] addition does not appear prohibitively high, however, when only a [2+2] reaction is possible. This agrees with experimental evidence that dienes form the [4+2] cycloaddition product[8,9] while alkenes form the [2+2] product.[7]

As expected, the barriers to these cycloaddition reactions are higher than those for the corresponding reactions on the Si(100) surface, but lower than those with molecular C−C double bonds. Calculations with the three-dimer model show that the [4+2] product on an extended terrace prefers a vertical, planar conformation as a consequence of repulsive interactions with an adjacent dimer. This is also a significant difference compared to Si(100) where experiment and theory agree that the [4+2] product is in a bent conformation. Repulsive interdimer interactions on the Si surface are weaker than those on diamond because of the greater interdimer distance.

Calculated IR spectra for the product species are a valuable tool in understanding the geometry of the adsorbed species, though in this case there is no clear agreement between the observed spectrum and the calculated spectrum for any single product. Our calculations are consistent with the presence of multiple conformations of the [4+2] product and a [2+2] side product. Our calculations also predict that the [2+2] reaction should not compete kinetically with the [4+2] reaction, though this was done with the single-dimer model of the surface. The difference in activation barriers may be modified by interdimer interactions or interadsorbate interactions, allowing the [2+2] reaction to compete more effectively.

Acknowledgment. We wish to thank Stacey Bent, John Russell, and their co-workers for several discussions about their work, and for making their vibrational spectra available. We also want to acknowledge the support of the National Science Foundation through grants CTS-9724404 and CHE-9971241.

JA002023J